Large dispersion of incoherent spectral features in highly ordered C_{60} chains

A. Tamai,[1,*] A. P. Seitsonen,[2,†] T. Greber,[1] and J. Osterwalder[1]
[1]*Physik Institut der Universität Zürich, Winterthurerstrasse 190, CH-8057 Zürich, Switzerland*
[2]*Physikalisch Chemisches Institut, Universität Zürich, Winterthurerstrasse 190, CH-8057 Zürich, Switzerland*
(Received 6 December 2005; revised manuscript received 17 May 2006; published 15 August 2006)

Ordered one-dimensional C_{60} chains on a vicinal Cu template were studied by angle-resolved photoemission. A complete structural model for C_{60} on Cu(553) is proposed, where two differently coordinated and oriented C_{60} molecules self-assemble in chains along the steps of the vicinal substrate. The highest occupied molecular orbital–derived peak shows a broad Gaussian line shape with features dispersing up to 400 meV along the chains. The line shape is interpreted in terms of a strong electron-phonon interaction leading to the formation of polarons with a spectral function dominated by incoherent multiphonon excitations. The large dispersion of this incoherent peak derives from a particularly favorable relative orientation of the molecules and is in good agreement with the one-electron band structure calculated by density functional theory, which indicates that the photoelectrons carry some memory of the frozen lattice.

DOI: 10.1103/PhysRevB.74.085407 PACS number(s): 71.20.Tx, 71.38.−k, 79.60.−i, 81.16.−c

I. INTRODUCTION

The fabrication of one-dimensional structures on surfaces is attracting considerable interest for possible applications in nanoelectronics.[1–3] If the electrons are confined to move along a single direction, correlations become more important and these systems are expected to show novel and exotic behaviors.[4] C_{60} chains are particularly interesting candidates for such studies because of the rich transport properties of the molecule in the solid phase, ranging from metallic to Mott-Hubbard insulating and superconducting behavior.[5]

Angle-resolved photoemission spectroscopy (ARPES) has evolved as the standard tool to map the electronic structure of complex solids. It is traditionally interpreted in a picture appropriate for weakly interacting systems, where Lorentzian peaks trace the dispersion of quasiparticlelike electronic states. This applies to the C_{60} lowest unoccupied molecular orbital (LUMO) in the metallic phase where the dispersion was found to be consistent with band structure calculations renormalized due to the coupling with high-energy phonons.[6] A different approach is necessary for a fully occupied molecular level such as the C_{60} highest occupied molecular orbital (HOMO). Gas phase experiments indicate that the photohole heavily couples to cage vibrational modes leading to the formation of polarons.[7–9] The resulting photoemission spectrum is dominated by incoherent multiphonon excitations and can be described by a series of discrete peaks in a Gaussian envelope. In a neutral C_{60} molecule the HOMO is a fivefold-degenerate fully occupied h_u orbital. In the solid state the energy levels split and the overlap of the orbitals broadens the levels to five electronic bands. For bulk C_{60}, a total bandwidth of 600 meV has been calculated within the local density approximation.[10] A dispersion of this magnitude should be clearly resolved in ARPES, whose energy and momentum resolution are far better. However, the reported experimental results are conflicting: Early ARPES data taken at very low photon energies, where final-state effects may be important, indicated a large bandwidth of up to 1 eV.[11,12] On the other hand, from angle-integrated photoemission it was estimated that the HOMO dispersion should be no larger than 70 meV, consistent with a large mass enhancement due to the formation of polarons.[7]

In this paper, we present a consistent picture of electronic excitations from the C_{60} HOMO in the solid state. Investigating one-dimensional molecular chains with ARPES, we find that the HOMO exhibits a broad Gaussian line shape with features following the one-electron bands calculated within density functional theory (DFT). The apparent inconsistency between a broad linewidth and a weakly renormalized dispersion is resolved by invoking a Franck-Condon-type model for the photoemission process, where the spectrum is dominated by incoherent weight representing transitions to various vibrationally excited final states. Recent calculations by Rösch and Gunnarsson showed that in this case the peak center of gravity traces the dispersion of the *frozen* lattice and does not reflect the quasiparticle velocity.[13] The actual quasiparticle has only negligible weight in the spectrum. Its dispersion can be estimated from the onset of the Gaussian envelope and is found to be consistent with a polaronic model for the HOMO.

II. EXPERIMENT

Experiments were performed in an UHV system, combining a Park VPII scanning tunneling microscope (STM) with a VG ESCALAB spectrometer, modified for fully automated angle-scanned x-ray and uv photoemission experiments.[14,15] X-ray photoelectron diffraction (XPD) has been performed using Mg $K\alpha$ radiation with the sample at room temperature. All ARPES data were taken at 21.22 eV photon energy (He $I\alpha$ radiation) using a monochromatized high-flux He discharge lamp. The resolution parameters were set to $\Delta E < 40$ meV and $\Delta\theta < 0.8°$ full width at half maximum (FWHM). Cu(553), the stepped surface used in this work, is a *B*-type vicinal of Cu(111) with $(11\bar{1})$ step facets. The nominal terrace width is 9.8 Å, which is close to the van der Waals diameter of the C_{60} molecules. The single crystal has been prepared and characterized as described in a previous publication.[16] C_{60} powder (99.9%) was sublimated from a titanium crucible onto the surface held at 600 K.

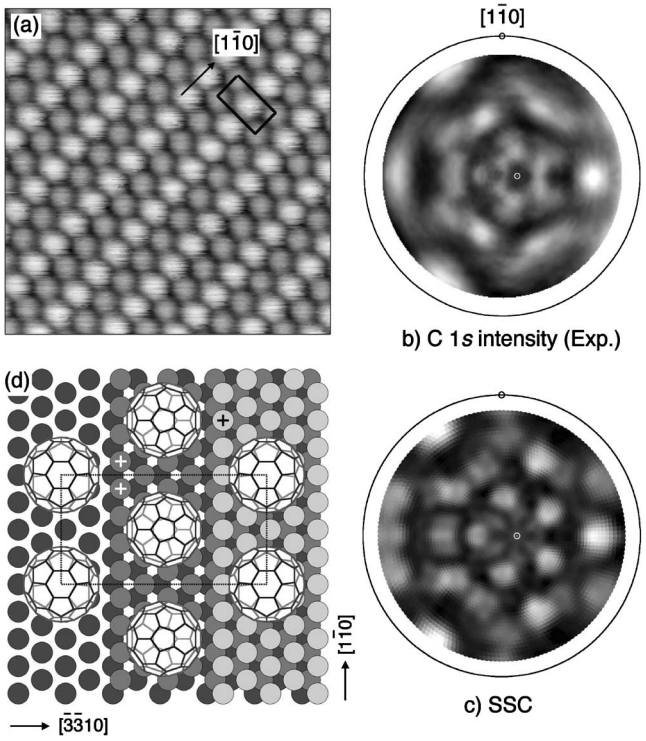

FIG. 1. (a) Room-temperature STM image (100×100 Å^2, −1.5 V sample bias, 1 nA tunneling current). (b) Experimental C 1*s* XPD pattern (Mg $K\alpha$, E_{kin}=970 eV). The direction of the substrate along the step and the terrace normal are indicated. (c) SSC calculations for pentagon- and hexagon-bonded C_{60} molecules superimposed with equal weight. (d) Suggested real space model for the C_{60} chains on the unit cell of Cu(553). Top view along [111]. The crossed markers show the different coordination to the copper atoms of the step for C_{60} molecules of adjoining chains.

III. RESULTS AND DISCUSSION

The structure of one monolayer of C_{60}/Cu(553) is described in Fig. 1. STM images show that the molecules form long chains of alternating brightness aligned along the step direction of the substrate [Fig. 1(a)]. The separation between the chains corresponds to a 4% expansion of the hexagonal pattern perpendicular to the steps. As discussed in Ref. 17, the size of the C_{60} unit cell and the type of vicinal surface (*B* type) imply two different C_{60} adsorption sites with different coordinations to the ascending steps. From the observation that C_{60} vacancies are more frequent in the bright chains it was conjectured that the molecules in the bright chains have a lower binding and coordination to the substrate. Further important structural information is provided by the successful interpretation of x-ray photoelectron diffraction patterns. The experimental C 1*s* XPD pattern from the ordered C_{60} monolayer is displayed in Fig. 1(b). The data were measured in the forward scattering regime (E_{kin}=970 eV) and are presented as a stereographic projection in a linear gray scale with maximum intensity corresponding to white. The pattern has been averaged exploiting the symmetry of the substrate perpendicular to the steps and normalized to a smooth polar-angle-dependent background typical for adsorbate emission. Figure 1(c) shows the result of single-scattering cluster

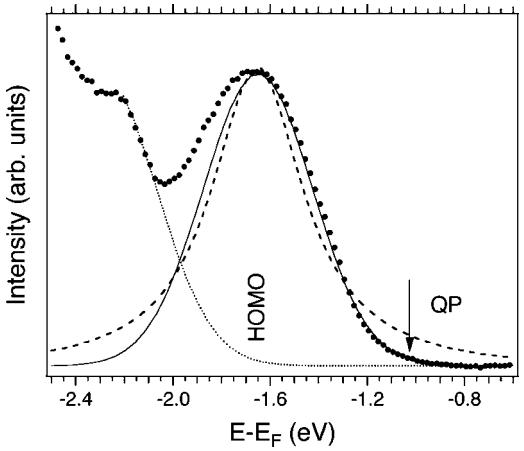

FIG. 2. Normal emission valence band spectrum with fits of the low-energy side of the HOMO peak to a Lorentzian (dashed line) and a Gaussian (full line).

(SSC) calculations for a superposition of C_{60} molecules adsorbed on a pentagon and on a hexagon ring, with the bonding normal to the (111) terraces. While the pentagon-bonded molecules have a single orientation, two symmetry-equivalent orientations of the hexagon-bonded molecules were considered. Comparing Figs. 1(b) and 1(c) it is seen that the experimental data are well described by these orientations since most of the prominent features in the XPD pattern are well reproduced in the calculation. The different STM contrast between the chains is thus consistent with the coexistence of two molecular orientations, where the higher density of states of the LUMO on the pentagon rings[18] suggests that the bright chains are the pentagon-bonded ones. A real space model of the dual chain structure is presented in Fig. 1(d).

Figure 2 shows a valence band normal emission spectrum from the one-dimensional ordered structure. Below 2 eV binding energy significant substrate emission from the Cu *d* bands is visible.[19] The C_{60} HOMO contributes a broad peak at 1.65 eV. In a coherent quasiparticle picture, the spectral function should be approximately Lorentzian with a width determined by the photohole lifetime. Interestingly, a fit of the low-energy side of the peak shows that the line shape of the HOMO compares far better with a Gaussian. Hybridization between Cu and C_{60} electronic states could probably justify the large width but not the line shape of the peak. This can be explained by the strong coupling between the h_u orbital and the low-energy vibrations of the C_{60} cage,[20] which leads to multiphonon excitations during the photoemission process. In this case, according to the Franck-Condon principle for molecular systems,[21] the spectral function consists of a series of discrete peaks, the intensities of which follow a Poisson distribution. When the number of excited phonons is large, the envelope function becomes a Gaussian,[22] in perfect agreement with the experimental line shape of the C_{60} HOMO. The coherent quasiparticle peak, which represents a transition without phonon excitations, should appear as a sharp feature at the onset of the Gaussian envelope but its spectral weight is completely suppressed. This behavior is in line with the formation of polarons, as suggested also for

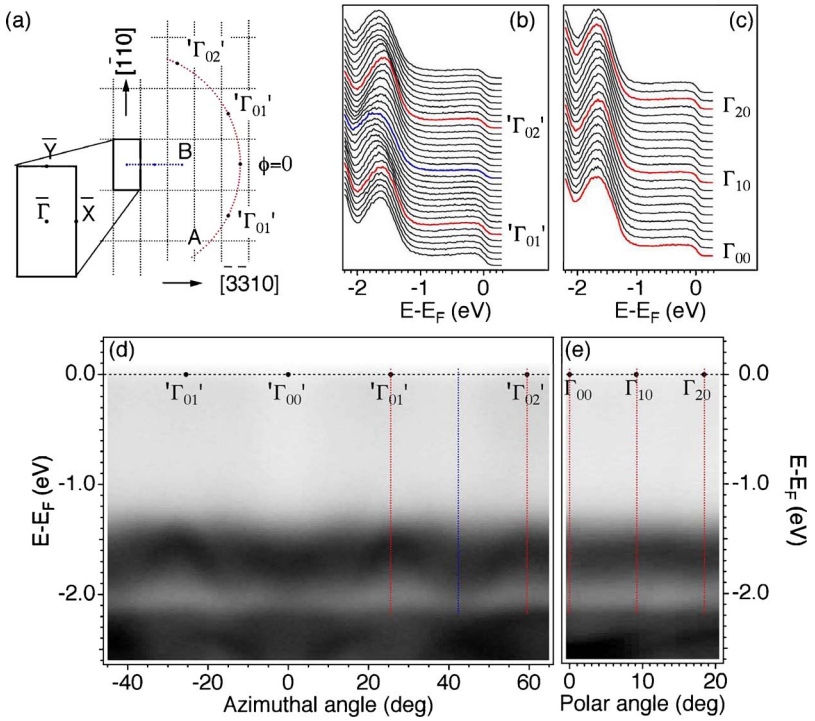

FIG. 3. (Color online) (a) Sketch of the C_{60} Brillouin zone and scan directions of the azimuthal cut *A* and the polar cut *B*, shown in (d) and (e), respectively. The azimuthal cut is measured at a polar angle of 44° around $[\bar{3}\bar{3}10]$ (ϕ=0°). The polar cut is along $[\bar{3}\bar{3}10]$, the direction perpendicular to the C_{60} chains. (b) and (c) Sets of energy distribution curves measured along the azimuthal cut *A* and along the polar cut *B*, respectively. (d) and (e) Angular intensity distribution maps along the azimuthal cut *A* and the polar cut *B*. The photoemission intensity is displayed on a linear gray scale with black at maximum intensity.

other systems where strong electron-phonon coupling is present.[23–26]

Figures 3(b) and 3(c) show single spectra at different emission angles along the azimuthal cut *A* and the polar cut *B* of Fig. 3(a). The azimuthal cut is measured at a polar angle of of 44° around $[\bar{3}\bar{3}10]$ (ϕ=0°) and it crosses the center of many C_{60} Brillouin zones. The polar cut is along $[\bar{3}\bar{3}10]$, the direction perpendicular to the C_{60} chains. Along the azimuthal scan there are changes in position and width of the broad HOMO peak that are indicative of dispersion, while perpendicular to the chains we observe only small variations of the peak position, as expected for a quasi-one-dimensional system. The angular intensity distribution maps of Figs. 3(d) and 3(e) show high intensity in a broad energy range between 1.4 and 1.9 eV. On top of it, along the azimuthal scan, a peak disperses at least 250 meV. The first zone is an exception since most probably around ϕ=0° there is a significant contribution of the Cu *sp* band, as confirmed by DFT calculations of the copper band structure performed using the linear augmented plane-wave method as implemented in the WIEN code.[27] The same HOMO dispersion was observed at a different photon energy (He *IIα* radiation). This makes it unlikely that the angular dependence of the C_{60}-derived peak is due to a final-state effect, i.e., dispersion of unoccupied bands with favorable matrix elements.[11,12]

The large dispersion of the HOMO is in contrast with the significant enhancement of the effective mass expected for the formation of polarons. In order to investigate the origin of these dispersing features we calculated the HOMO band structure for a free-standing C_{60} layer within density functional theory in the local density approximation (DFT-LDA) (Fig. 4). First, we consider only chains with a unique molecular orientation: molecules adsorbed on the pentagon (a) and on the hexagon (b) according to the XPD pattern. The calculations show that the relative molecular orientation is a very sensitive parameter: Along the chains, the total bandwidth is 350 meV for molecules lying on the pentagon, while all other orientations we considered gave smaller values. For molecules adsorbed on the hexagon, the bandwidth is only 170 meV. Figure 4(c) displays the HOMO dispersion for the experimental chain structure with two C_{60} molecules in the

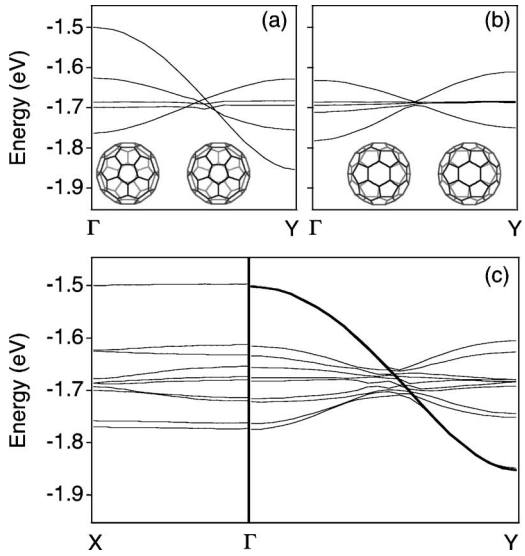

FIG. 4. DFT-LDA calculations of the h_u (HOMO) band structure for C_{60} chains in a free-standing layer. The distance between the molecules is set to the experimental values. The energy scale has been shifted for a comparison with the experiment (see text). (a) and (b) Chains of molecules sitting on the pentagon and on the hexagon, respectively. Insets: top view along the chains. (c) Band dispersion for the dual chain structure. The solid line emphasizes the band with the largest dispersion.

unit cell. Along the chains ($\bar{\Gamma}\bar{Y}$) the dispersion is very similar to a simple superposition of the two orientations (a) and (b). Perpendicular to the chains ($\bar{\Gamma}\bar{X}$) the bands are rather flat with a dispersion of up to 25 meV. The clear anisotropy between the two directions indicates, in agreement with the experiments, that the electronic coupling between the molecules occurs predominantly along the chains. The pronounced one-dimensional character can be due to the 4% increased distance between the chains and/or to the different molecular orientations. These two aspects of the structure have a dramatic effect on the intermolecular hopping because of the high angular momentum ($L=5$) of the HOMO and because it is built of $2p$ orbitals that point radially out of the cage and decay very rapidly with the distance.[5,28,29] Band structure calculations for different geometries of the unit cell indicate that the larger distance between the molecules in the perpendicular direction is the main cause of the quasi-one-dimensional dispersion.

Pentagon-bonded C_{60} molecules have never been observed so far in monolayer systems on low-index metal surfaces,[30] and their formation might be related to the coordination of the molecules to the substrate step. Total energy calculations for a two-dimensional free-standing layer of C_{60} chains indicate that chains of molecules with a hexagon ring parallel to the layer (hexa) as depicted in Fig. 4(b) are more stable than those with a pentagon ring parallel to the layer (penta) [Fig. 4(a)]. With respect to the hexa structure, the total energy for alternating chains of pentagon- and hexagon-bonded molecules is 25 meV/C_{60} higher and for pentagon-bonded chains it is 49 meV/C_{60} higher. The facts that theory favors for free-standing layers hexa chains and that the experiment indicates alternating penta-hexa chains for C_{60} on Cu(553) signal an active role of the substrate for the formation of this peculiar molecular arrangement.

Following a Franck-Condon-type model for the photoemission process, for each of the ten HOMO bands of Fig. 4(c) we would expect one broad Gaussian peak due to incoherent multiphonon excitations and at the onset of intensity one quasiparticle peak. The true quasiparticle dispersion for each band is very difficult to extract because of the low spectral weight. However, the momentum dependence of the peak width indicates small dispersion at the onset of the HOMO. Figure 5 shows that the width $\Gamma(\mathbf{k})$ of the overall Gaussian envelope increases directly proportional to the peak position $\epsilon(\mathbf{k})$. This linear behavior cannot be explained as the combined effect of the ten bands dispersing according to DFT [Fig. 4(c)], nor by a different chemical potential or charge state of the two chains (see below). It is rather interpreted as an intrinsic property of the peak line shape. The same effect has been reported for the undoped cuprates in the polaronic regime.[24] In that case, recent spectral function calculations for strong electron-phonon coupling confirm the dependence of the width on the binding energy.[31] A tentative position of the quasiparticle peak has been derived from the position $\epsilon(\mathbf{k})$ and the FWHM $\Gamma(\mathbf{k})$. In Fig. 6(b) this is done by mapping the onset of the peak at $\epsilon(\mathbf{k})+\Gamma(\mathbf{k})$, where the intensity has decayed to 1% of the maximum. The quasiparticle peak is around 1.1 eV and disperses less than 50 meV, which is consistent with a polaronic model for the HOMO.

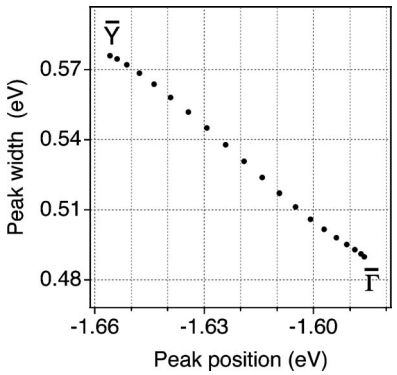

FIG. 5. HOMO width $\Gamma(\mathbf{k})$ (FWHM) as a function of the peak position $\epsilon(\mathbf{k})$ from $\bar{\Gamma}$ to $\bar{Y}$.

At higher energy the photoemission intensity is dominated by incoherent excitations. In order to disentangle the contribution of the different bands, we performed a fit to the angle resolved spectra with Gaussian functions [Figs. 6(a) and 6(b)]. We obtain a good fit with two components with a fixed relative weight of 9:1 [Fig. 6(a)]. The first component disperses very little around 1.61 eV and it is interpreted as the combined signature of the nine bands that according to the calculation have bandwidths smaller than 200 meV. The second component shows dispersion up to 400 meV. In order to compare these results with the DFT band structure, the latter has been shifted in energy to align the band with largest dispersion [solid line in Fig. 3(c)] to the second component. The position of the Gaussian traces the dispersion of the DFT band with excellent agreement. This has also been observed in the undoped cuprates, where the dispersion of a broad peak matches the quasiparticle dispersion calculated in purely electronic models.[24] The position of the first Gaussian, which corresponds to the center of gravity of the nine bands, is then 80 meV lower in energy than in the calculation. This shift can indicate a different position of the chemical potential for the two C_{60} chains. Charge transfer from the substrate to the molecule in the order of one electron per C_{60} has been reported on Cu(111),[19,32] and different electron dop-

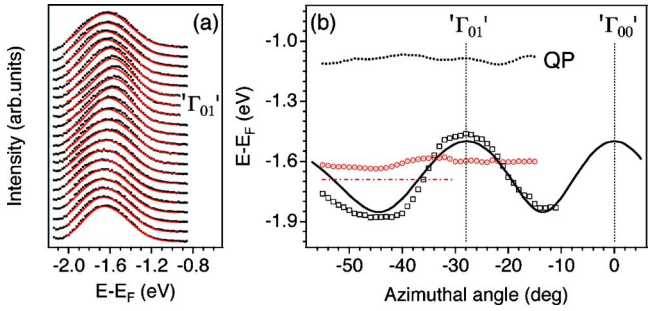

FIG. 6. (Color online) (a) Fit to the angle-resolved spectra with two Gaussian components after background subtraction. (b) Quasiparticle (QP) dispersion as determined by the onset of the peak (dots). Positions of the two Gaussians from the fit (squares and circles). The dash-dotted line indicates the center of gravity of the nine DFT bands that disperse less than 200 meV. The DFT band with the largest dispersion is projected on the same azimuthal scan (full line).

ing can be expected for the two C_{60} chains, because the bonding geometry to the substrate is not the same [Fig. 1(d)]. A second possible reason for the shift in energy is that the electric field at the interface not only induces charge carriers but also polarizes the molecules and produces a significant splitting of the molecular levels (Stark effect). Wehrli *et al.* calculated the splitting of the HOMO for an electric field strong enough to transfer 1 e/C_{60}.[33] When the field is along the C_{5v} and the C_{3v} axes of the molecule, the expected Stark splitting is around 55 and 30 meV, respectively. If the field is along the C_{5v} axis, i.e., molecules with the pentagon ring facing the surface, four levels move to lower and one to higher binding energy, which is consistent with the experiment.

IV. CONCLUSIONS

We have presented the quasi-one-dimensional electronic structure of C_{60} chains grown on a vicinal template. Large dispersion of the HOMO derives from a particularly favorable relative orientation of the molecules along the chains. Following a Franck-Condon-type model for the photoemission process, the broad Gaussian line shape of the HOMO is interpreted as the incoherent part of the spectrum. Its dispersion follows the one-electron band structure in agreement with recent calculations.[13] Weak dispersion at the onset of the HOMO peak is compatible with a strongly renormalized quasiparticle due to the formation of polarons. These results represent a comprehensive picture of electronic excitations from a fully occupied molecular level and can be applied to other systems with strong electron-phonon coupling, such as the C_{60} LUMO in the insulating K_4C_{60} and K_6C_{60} phases.[23]

ACKNOWLEDGMENTS

We would like to thank O. Gunnarsson, M. Sigrist, S. Wehrli, M. Hengsberger, and F. Baumberger for fruitful discussions. This work was supported by the Swiss National Science Foundation.

*Present address: School of Chemistry and Centre for Science at Extreme Conditions, University of Edinburgh, Edinburgh EH9 3JZ, UK. Electronic address: anna.tamai@ed.ac.uk

†Present address: CNRS & IMPCMC, Université Pierre et Marie Curie, 4 place Jussieu, F-75252 Paris, France.

[1] F. J. Himpsel, K. N. Altman, R. Bennewitz, J. N. Crain, A. Kirakosian, J.-L. Lin, and J. L. McChesney, J. Phys.: Condens. Matter **13**, 11097 (2001).

[2] S. Lukas, G. Witte, and Ch. Wöll, Phys. Rev. Lett. **88**, 028301 (2002).

[3] R. Otero, Y. Naitoh, F. Rosei, P. Jiang, P. Thostrup, A. Gourdon, E. Loegsgaard, I. Stensgaard, C. Joachim, and F. Besenbacher, Angew. Chem. **116**, 2144 (2004).

[4] J. Voit, J. Electron Spectrosc. Relat. Phenom. **117**, 469 (2001).

[5] O. Gunnarsson, *Alkali-Doped Fullerides: Narrow-Band Solids with Unusual Properties* (World Scientific, Singapore, 2004).

[6] W. L. Yang *et al.*, Science **300**, 303 (2003).

[7] P. A. Brühwiler, A. J. Maxwell, P. Baltzer, S. Andersson, D. Arvanitis, L. Karlsson, and N. Martensson, Chem. Phys. Lett. **279**, 85 (1997).

[8] S. E. Canton, A. J. Yencha, E. Kukk, J. D. Bozek, M. C. A. Lopes, G. Snell, and N. Berrah, Phys. Rev. Lett. **89**, 045502 (2002).

[9] N. Manini, P. Gattari, and E. Tosatti, Phys. Rev. Lett. **91**, 196402 (2003).

[10] N. Laouini, O. K. Andersen, and O. Gunnarsson, Phys. Rev. B **51**, 17446 (1995).

[11] G. Gensterblum *et al.*, Phys. Rev. B **48**, 14756 (1993).

[12] P. J. Benning, C. G. Olson, D. W. Lynch, and J. H. Weaver, Phys. Rev. B **50**, 11239 (1994).

[13] O. Rösch and O. Gunnarsson, Eur. Phys. J. B **43**, 11 (2005).

[14] T. Greber, O. Raetzo, T. J. Kreutz, P. Schwaller, W. Deichmann, E. Wetli, and J. Osterwalder, Rev. Sci. Instrum. **68**, 4549 (1997).

[15] W. Auwärter, T. J. Kreutz, T. Greber, and J. Osterwalder, Surf. Sci. **429**, 229 (1999).

[16] F. Baumberger, T. Greber, and J. Osterwalder, Phys. Rev. B **64**, 195411 (2001).

[17] A. Tamai, W. Auwärter, C. Cepek, F. Baumberger, T. Greber, and J. Osterwalder, Surf. Sci. **566**, 633 (2004).

[18] M. Muntwiler, W. Auwarter, A. P. Seitsonen, J. Osterwalder, and T. Greber, Phys. Rev. B **71**, 241401(R) (2005).

[19] K.-D. Tsuei, J.-Y. Yuh, C.-T. Tzeng, R.-Y. Chu, S.-C. Chung, and K.-L. Tsang, Phys. Rev. B **56**, 15412 (1997).

[20] N. Manini, A. Dal Corso, M. Fabrizio, and E. Tosatti, Philos. Mag. B **81**, 793 (2001).

[21] P. H. Citrin, G. K. Wertheim, and Y. Baer, Phys. Rev. B **16**, 4256 (1977).

[22] G. Mahan, *Many-Particle Physics* (Plenum, New York, 1981).

[23] S. Wehrli, T. M. Rice, and M. Sigrist, Phys. Rev. B **70**, 233412 (2004).

[24] K. M Shen *et al.*, Phys. Rev. Lett. **93**, 267002 (2004).

[25] L. Perfetti, S. Mitrovic, G. Margaritondo, M. Grioni, L. Forro, L. Degiorgi, and H. Hochst, Phys. Rev. B **66**, 075107 (2002).

[26] D. S. Dessau, T. Saitoh, C.-H. Park, Z.-X. Shen, P. Villella, N. Hamada, Y. Moritomo, and Y. Tokura, Phys. Rev. Lett. **81**, 192 (1998).

[27] P. Blaha, K. Schwarz, and J. Luitz, *WIEN97, A Full Potential Linearized Augmented Plane Wave Package for Calculating Crystal Properties* (Karlheinz Schwarz Techn. Univesitaet Wien, Austria, 1999).

[28] V. Brouet, W. L. Yang, X. J. Zhou, H. J. Choi, S. G. Louie, M. L. Cohen, A. Goldoni, F. Parmigiani, Z. Hussain, and Z.-X. Shen, Phys. Rev. Lett. **93**, 197601 (2004).

[29] A. Tamai, A. P. Seitsonen, R. Fasel, Z.-X Shen, J. Osterwalder, and T. Greber, Phys. Rev. B **72**, 085421 (2005).

[30] R. Fasel, P. Aebi, R. G. Agostino, D. Naumovic, J. Osterwalder, A. Santaniello, and L. Schlapbach, Phys. Rev. Lett. **76**, 4733 (1996).

[31] O. Rösch, O. Gunnarsson, X. J. Zhou, T. Yoshida, T. Sasagawa, A. Fujimori, Z. Hussain, Z.-X. Shen, and S. Uchida, Phys. Rev. Lett. **95**, 227002 (2005).

[32] Lin-Lin Wang and Hai-Ping Cheng, Phys. Rev. B **69**, 045404 (2004).

[33] S. Wehrli, E. Koch, and M. Sigrist, Phys. Rev. B **68**, 115412 (2003).